Bioelectrochemistry 91 (2013) 32–36

Contents lists available at SciVerse ScienceDirect

Bioelectrochemistry

journal homepage: www.elsevier.com/locate/bioelechem

The application of chiral arginine and multi-walled carbon nanotubes as matrices to monitor hydrogen peroxide

Qiao Chen [a], Min Chen [b], Juan Zhou [a], Qian Han [a], Yonghua Wang [a], Yingzi Fu [a,*]

[a] Key Laboratory on Luminescence and Real-Time Analysis, Ministry of Education, College of Chemistry and Chemical Engineering, Southwest University, Chongqing 400715, PR China
[b] Rongchang School, Chongqing 402460, PR China

ARTICLE INFO

Article history:
Received 13 June 2012
Received in revised form 28 December 2012
Accepted 30 December 2012
Available online 12 January 2013

Keywords:
Multi-walled carbon nanotubes
Arginine enantiomers
Horseradish peroxidase
Enantioselective recognition

ABSTRACT

The enantioselective interaction between horseradish peroxidase (HRP) and arginine enantiomers was investigated by electrochemical methods through studying the electrocatalytic activity of H_2O_2 biosensor, which was obtained through L-arginine or D-arginine functionalized multi-walled carbon nanotubes (D-Arg-MWCNTs or L-Arg-MWCNTs) immobilizing horseradish peroxidase (HRP) on glassy carbon electrode. Cyclic voltammetric and chronoamperometry were used to characterize the properties of the biosensor. Under the optimal conditions, LAM-CS@HRP/dpAu/GCE biosensor showed better electrocatalytic activity to H_2O_2 compared to DAM-CS@HRP/dpAu/GCE and MWCNTs-CS@HRP/dpAu/GCE, implying that the different configurations of nanocomposites have different interactions with HRP. The currents of LAM-CS@HRP/dpAu/GCE biosensor had a linear relationship with the concentration of H_2O_2 in the range of 2.5×10^{-6} to 2.9×10^{-3} M with a detection limit of 8.3×10^{-7} M (S/N = 3). For MWCNTs-CS-HRP/dpAu/GCE electrode, the calibration range of H_2O_2 was from 6.4×10^{-4} to 2.9×10^{-2} M and a detection limit of 2×10^{-5} M (S/N = 3). For the case of DAM-CS@HRP/dpAu/GCE, there has a linear relationship with the concentration of H_2O_2 from 1.8×10^{-5} to 2.6×10^{-3} M and the detection limit is 6×10^{-5} M (S/N = 3).

1. Introduction

The existence and induction of chirality are one of the most intriguing and inspiring phenomena in nature [1,2]. Living beings are composed of a variety of optically active macromolecules, in which chiral recognition plays a crucial role for maintaining their function [3,4]. The body exhibits different physiological responses to stimuli caused by enantiomers of a racemic drug, which may have different pharmacological activities, pharmacokinetic and pharmacodynamic effects [5–7]. With the increasing use of chiral compounds in pharmaceuticals and agrochemicals, the detection of chiral compounds still remains an important subject [8].

Amino acids are important biological compounds. Different configurations of amino acids differ in their biological or physiological activities [9]. L-forms amino acids play an important role in the food and pharmaceutical industries, while D-forms were discovered in species of lower animals, vegetables and fruits [10–12], and D-amino acids are generally considered to be important markers of bacterial contamination of food products [13]. Great efforts have been made to discriminate amino acids enantiomers [14–16]. Arginine (Arg) is frequently used in structural probing of proteins and RNA based on the guanidino group is the excellent recognition sites to bio-molecules [17]. L-Arg is a precursor of nitric oxide and protein synthesis, and it plays a very important role in the living systems [18,19]. While D-Arg, an active molecule in mammals, is believed to have pharmacological activity [20]. Therefore, developing the methods for the recognition of Arg enantiomers is lasting and interesting.

The electronic properties of multi-walled carbon nanotubes (MWCNTs), which are the subtle electronic properties, the excellent conductivity, the high aspect ratio, the large specific area and good chemical stability, suggested that they have the ability to mediate the electron-transfer reactions and can be exploited as a mean of promoting the reactions in a wide range of bioactive species [21–26]. Functionalized MWCNTs have been widely used in constructing biosensor for the good physical properties and solubility [27–29]. Chiral molecular functionalized MWCNTs, which could keep the chirality and excellent electronic properties, are potential biomaterials applied in biosensor.

In this work, Arg enantiomers functionalized MWCNTs and MWCNTs were used to construct hydrogen peroxide (H_2O_2) biosensor. Compared DAM-CS@HRP/dpAu/GCE or LAM-CS@HRP/dpAu/GCE with MWCNTs-CS@HRP/dpAu/GCE, LAM-CS@HRP/dpAu/GCE has the best electrocatalytic effect toward the reduction of H_2O_2. The difference of electrocatalytic activity of DAM@HRP/dpAu/GCE and LAM-CS@HRP/dpAu/GCE may be caused by the enantioselective interaction between HRP and Arg enantiomers. This work not only provides a new method for investigating the enantioselective interaction of chiral molecules and biomolecules, but also constructs a new biosensor for the detection of H_2O_2.

* Corresponding author. Tel.: +86 023 68252360; fax: +86 023 6825.
E-mail address: fyzc@swu.edu.cn (Y. Fu).

1567-5394/$ – see front matter © 2013 Elsevier B.V. All rights reserved.
http://dx.doi.org/10.1016/j.bioelechem.2012.12.003

2. Experimental

2.1. Reagents and materials

The multi-walled carbon nanotubes (MWCNTs > 95%), L- and D-arginine (L- and D-Arg, 98%) were purchased from Chengdu Organic Chemicals Co., Ltd. (Chengdu, China). Gold chloride ($HAuCl_4$), chitosan (CS), *N*-hydroxy succinimide (NHS), *N*-(3-dimethylaminopropyl)-N′-ethylcarbodiimidehydrochloride (EDC) and Horseradish peroxidase (HRP) were purchased from Sigma Chemical Co. (St. Louis, USA). Hydrogen peroxide (H_2O_2, 30%) was purchased from Chemical Reagent Co. (Chongqing, China). Various pH of phosphate buffer solutions (PBS) containing 0.1 M KCl were prepared by 0.1 M of KH_2PO_4 and 0.1 M of Na_2HPO_4. Other chemical reagents were analytical grade and used without further purification. Double distilled water was used throughout the study. All the experiments were carried out at room temperature (25.0 ± 0.5 °C).

2.2. Apparatus

Cyclic voltammetric (CV) and chronoamperometry measurements were performed on a CHI 660D electrochemistry workstation (Shanghai Chenhua Instruments Co., China). A conventional three-electrode system was employed with bare or the modified electrodes as the working electrodes, a platinum wire auxiliary electrode as the counter electrode and a saturated calomel reference electrode (SCE) as the reference electrode.

2.3. Constructing the chiral hydrogen peroxide biosensors

L- or D-Arg functionalized MWCNTs were obtained as follows. First, the oxidized MWCNTs were added into NHS solution and sonicated. Then EDC was added in the stirred mixture and allowed to react for 3 h. After that, the obtained solution was successively centrifuged and rinsed thoroughly with water. Next, it was transferred to L- or D-Arg solution, the L- or D-Arg functionalized MWCNTs were obtained by covalent interaction between the $-NH_2$ of Arg and –COOH of the MWCNTs [30].

Before each experiment, GCEs (Φ = 4 mm) were polished with 1.0, 0.3, and 0.05 μm of alumina slurries, which was followed by successive sonicating in water, and ethanol. Then, the cleaned GCEs were immersed in 1% $HAuCl_4$ solution, and treated by controlling −0.2 V for 1 min to get gold nanocrystal film (dpAu/GCE) [31,32]. 0.2 mg of D-Arg-MWCNTs or L-Arg-MWCNTs was dispersed in 0.6 mL of CS by sonicating for 1 h, then HRP (0.4 mg/mL) was added and sonicated for 0.5 h to obtain a stable black suspension. 10 μL of the suspension was dropped on the surface of the dpAu/GCE to fabricate a biosensor (noted LAM-CS@HRP/dpAu/GCE or DAM-CS@HRP/dpAu/GCE). For comparison, MWCNTs-CS@HRP/dpAu/GCE were also prepared by dropping 10 μL of MWCNTs-CS@HRP mixed solution on the dpAu/GCE, and dried in air at room temperature.

3. Results and discussion

3.1. Electrochemical characterization of the modified electrode

Cyclic voltammograms (CVs) of different modified electrodes were performed in 2.5 mM $[Fe(CN)_6]^{4-/3-}$ solution (pH 6.0) from −0.2 to 0.6 V at a scan rate of 0.05 V/s. As shown in Fig. 1, a standard redox peak was observed on the bare GCE (curve a). After the GCE electrode deposited with the $HAuCl_4$, the peak current increased because of good electronic transmission of gold nanoparticles (curve b). When LAM-CS@HRP or DAM-CS@HRP mixture modified on dpAu/GCE, a further increase of the peak current was obtained and the peak current values of LAM-CS@HRP/dpAu/GCE and DAM-CS@HRP/dpAu/GCE were almost the same (curve c and c′), which is due to good conductive properties of chiral nanotubes.

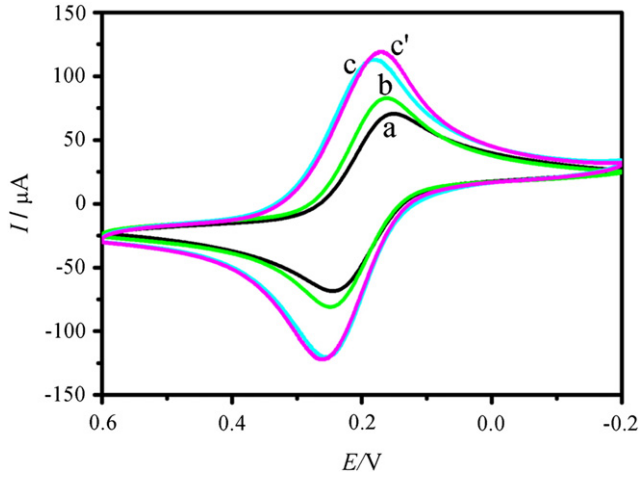

Fig. 1. Cyclic voltammograms of different electrodes. (a) GCE; (b) dpAu/GCE; (c) DAM-CS@HRP/dpAu/GCE; (c′) LAM-CS@HRP/dpAu/GCE in 2.5 mM $[Fe(CN)_6]^{4-/3-}$ solution at 50 mV/s.

The CV performance of LAM-CS@HRP/dpAu/GCE and DAM-CS@HRP/dpAu/GCE electrodes at different scan rates was measured. Both the anodic and cathodic peak currents were directly proportional to the square root of scan rate ($v^{1/2}$) from 0.02 to 0.50 V/s, suggesting diffusion controlled electron transfer process.

3.2. Optimization of analytical conditions

3.2.1. The influence of pH

The pH of the working buffer is an important influencing factor for the sensitivity of the modified electrode. To improve the performance of the biosensor, the optimum pH for modified electrode was selected by amperometric response in a series of PBS (containing 0.2 mM H_2O_2) from 4.8 to 8.0. As shown in Fig. 2A, the amperometric response of both LAM-CS@HRP/dpAu/GCE (a) and DAM-CS@HRP/dpAu/GCE (b) increases the pH value from 4.8 to 6.0, and then decreases. The amperometric currents achieved the highest value at pH 6.0, which indicated that pH 6.0 was optimum. The reason might be that the bioactivity of HRP would decrease in a strong acidic or alkaline solution. So, the buffer solution of pH 6.0 was selected for further experiments. In addition, it can also be seen that the catalytic reduction of H_2O_2 on LAM-CS@HRP/dpAu/GCE electrode was always larger than DAM-CS@HRP/dpAu/GCE.

3.2.2. The effect of applied potential

The effect of applied potential on the amperometric response of the modified electrodes toward H_2O_2 (0.2 mM) was also investigated on the applied potential from −0.05 V to −0.50 V. As shown in Fig. 2B, the peak current of LAM-CS@HRP/dpAu/GCE (a) and DAM-CS@HRP/dpAu/GCE (b) was gradually increasing with applied potential varies from −0.05 V to −0.50 V. Considering the interference of many coexisted foreign species at too negative potential, −0.25 V was chosen as the working potential to maintain a high sensitivity.

3.3. Electrocatalytic performance of the chiral biosensor

Fig. 3A displayed electrocatalytic activity of the LAM-CS@HRP/dpAu/GCE (I) and DAM-CS@HRP/dpAu/GCE (II) toward the reduction of H_2O_2 at a scan rate of 0.05 V/s. Curve a was the CV in the absence of H_2O_2, after H_2O_2 was added into the PBS (pH 6.0), an obvious increase in the peak current was observed (curve b). The results show that LAM-CS@HRP and DAM-CS@HRP have successful modification on dpAu/GCE. And the chiral nanocomposites have good biocompatibility which can maintain the biological activity of HRP. It is noteworthy that the catalytic effects of LAM-CS@HRP/dpAu/GCE were better than

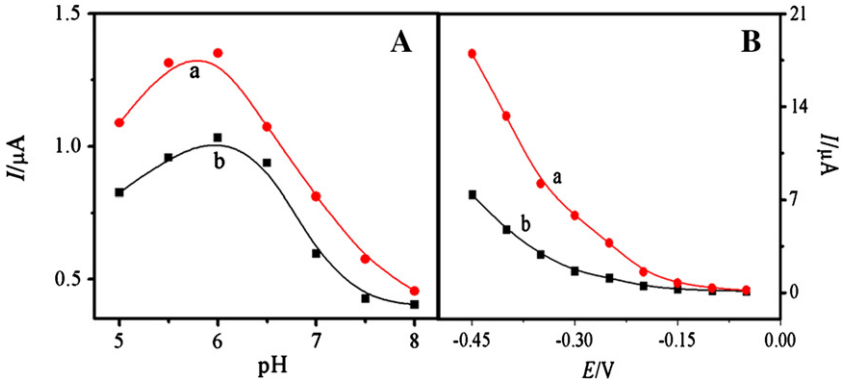

Fig. 2. Effects of pH (A) and applied potential (B) on steady-state response current to 0.2 mM H_2O_2. (a) LAM-CS@HRP/dpAu/GCE electrode and (b) DAM-CS@HRP/dpAu/GCE.

DAM-CS@HRP/dpAu/GCE. The oxidated process of H_2O_2 on LAM-CS@HRP/dpAu/GCE and DAM-CS@HRP/dpAu/GCE was shown in Fig. 3B.

To further investigate the roles of the chiral nanocomposites in the catalytic effects of H_2O_2, the chronoamperometry responses of LAM-CS@HRP/dpAu/GCE, DAM-CS@HRP/dpAu/GCE and MWCNTs-CS@HRP/dpAu/GCE were compared by successive injections of H_2O_2 to a continuous stirring of PBS solution (pH 6.0) at applied potential of −0.25 V. As shown in Fig. 4, the chronoamperometry response of LAM-CS@HRP/dpAu/GCE (a) was larger than that of MWCNTs-CS@HRP/dpAu/GCE (b) and DAM-CS@HRP/dpAu/GCE (c), and the difference of chronoamperometry response gradually increase with the increasing of H_2O_2 concentration.

Fig. 5 displayed the calibration curve of the biosensor for H_2O_2 determination. As can be seen, the LAM-CS@HRP/dpAu/GCE electrode displays a linear H_2O_2 concentration in the range from 2.5×10^{-6} to 2.9×10^{-3} M with a correlation coefficient of 0.998, and the detection limit is 8.3×10^{-7} M (S/N = 3) (a). For MWCNTs-CS-HRP/dpAu/GCE electrode, a linear range from 6.4×10^{-4} to 2.9×10^{-2} M is obtained with a correlation coefficient of 0.963, and the detection limit is 2×10^{-5} M (b). For the case of DAM-CS@HRP/dpAu/GCE, there has a linear relationship with the concentration of H_2O_2 from 1.8×10^{-5} to 2.6×10^{-3} M, with a correlation coefficient of 0.973, and the detection limit is 6×10^{-5} M (c). From above dates, it shows that the catalytic effect of LAM-CS@HRP/dpAu/GCE electrode is stronger than that of MWCNTs-CS@HRP/dpAu/GCE and DAM-CS@HRP/dpAu/GCE.

Compared to MWCNTs-CS-HRP/dpAu/GCE, the electrocatalytic behavior of HRP was improved upon its immobilization on the LAM-CS@HRP/dpAu/GCE, allowing an efficient electron transfer between the redox active site of the enzyme and the electrode surface, while the chronoamperometry response was decreased in the presence of D-Arg. The difference of chronoamperometry response between LAM-CS@HRP/dpAu/GCE and DAM-CS@HRP/dpAu/GCE may be resulting from

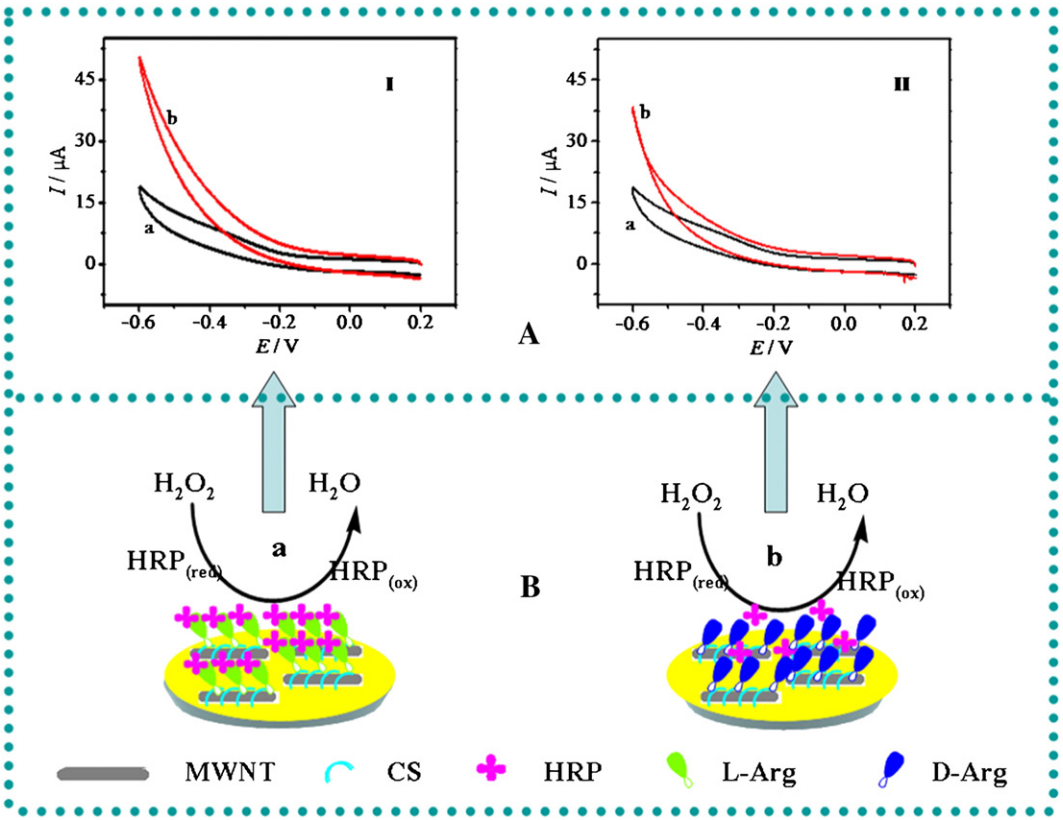

Fig. 3. A: The electrocatalytic activity of the LAM-CS@HRP/dpAu/GCE (I) and the DAM-CS@HRP/dpAu/GCE (II) toward the reduction of H_2O_2. (a) in 0.1 M PBS (pH 6.0) without H_2O_2 and (b) in 0.584 mM H_2O_2 PBS (pH 6.0) at a scan rate of 0.05 V/s. B: The schematic representation of electrocatalysis progress of modified electrode to H_2O_2. (a) LAM-CS@HRP/dpAu/GCE and (b)DAM-CS@HRP/dpAu/GCE.

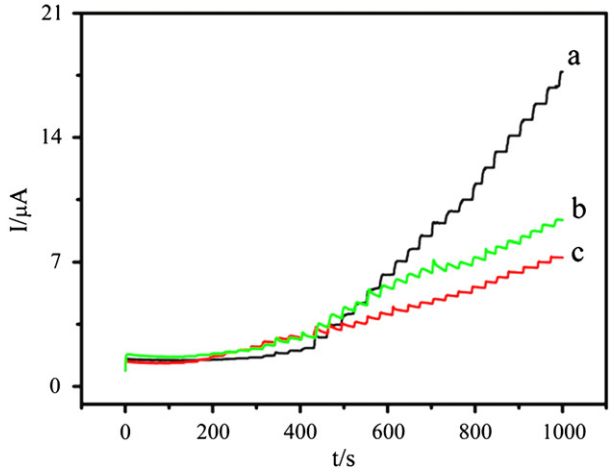

Fig. 4. Amperometric response of the different electrodes. (a) LAM-CS@HRP/dpAu/GCE; (b) MWCNTs-CS@HRP/dpAu/GCE and (c) DAM-CS@HRP/dpAu/GCE in PBS (pH 6.0) at an applied potential of −0.25 V upon successive additions of H_2O_2.

the chirality-induced difference in the molecular configurations for L- and D-Arg molecules, which greatly influences their interactions with HRP molecules. The spatial structure of L-Arg may match well with HRP and leads electron to transfer more easily than D-Arg.

3.4. Stability, repeatability and reproducibility of biosensors

The stability of the biosensors was studied. When the 100 continuous cyclic scans were carried out in the potential range from 0.6 to −0.2 V with a 0.05 V/s scan rate, the decrease of anodic current peaks was 1.8% for LAM-CS@HRP/dpAu/GCE, and 1.6% for DAM-CS@HRP/dpAu/GCE. On the other hand, after the modified chiral electrodes were stored at 4 °C for two weeks, the sensor retained 92% (DAM-CS@HRP/dpAu/GCE) or 90% (LAM-CS@HRP/dpAu/GCE) of its initial activity. It showed that this biosensor exhibited a high stability. The repeatability of the LAM-CS@HRP/dpAu/GCE biosensor and DAM-CS@HRP/dpAu/GCE biosensor was also investigated and relative standard deviation (RSD) was 3.2% and 3.8% (n = 6) for 0.2 mM H_2O_2. The reproducibility was determined in the presence of 0.2 mM H_2O_2. The RSD of the LAM-CS@HRP/dpAu/GCE biosensor and DAM-CS@HRP/dpAu/GCE biosensor was 4.5% and 4.7%, respectively. The good reproducibility may be due to the HRP molecules that were firmly immobilized on the electrode surface and the good biocompatibility of Arg enantiomers functionalized MWCNTs.

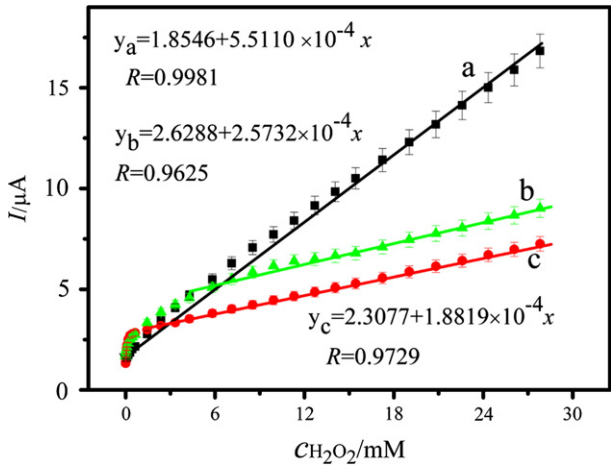

Fig. 5. Linear calibration curves. (a) LAM-CS@HRP/dpAu/GCE; (b) MWCNTs-CS@HRP/dpAu/GCE and (c) DAM-CS@HRP/dpAu/GCE.

4. Conclusions

The stereoselective interaction between the Arg enantiomers and HRP was investigated by electrochemical methods. The result shows that LAM-CS@HRP/dpAu/GCE, MWCNT-CS@HRP/GCE and DAM-CS@HRP/dpAu/GCE effectively retain electrocatalytic activity of HRP for the reduction of H_2O_2, but LAM-CS@HRP/dpAu/GCE biosensors show wider linear range, lower detection limit and good sensitivity for H_2O_2 than the others. The difference of electrocatalytic activity between LAM-CS@HRP/dpAu/GCE and DAM-CS@HRP/dpAu/GCE may be caused by the chirality of Arg. That is to say, HRP can selectively recognize Arg enantiomers and the spatial structure of L-Arg may match well with HRP and leads electron to transfer more easily than D-Arg. Based on this, it would be a good alternative method to further study the properties of biomacromolecule and the origin of the high chiral preference in nature. The developed chiral amino acid functionalized nanomaterials have a wide range of applications in biosensors.

Acknowledgment

This work was supported by the National Natural Science Foundation of China nos. 20972128 and 21272188.

References

[1] J. Zhang, A. Gesquière, M. Sieffert, M. Klapper, K. Müllen, F.C. De Schryver, S. De Feyter, Losing the expression of molecular chirality in self-assembled physisorbed monolayers [J], Nano Lett. 5 (2005) 1395–1398.
[2] E. Yashima, K. Maeda, Chirality-responsive helical polymers [J], Macromolecules 41 (2008) 3–12.
[3] P.H. Lin, S.J. Tong, S.R. Louis, Y. Chang, W.Y. Chen, Thermodynamic basis of chiral recognition in a DNA aptamer[J], Phys. Chem. Chem. Phys. 11 (2009) 9744–9750.
[4] I. Yagi, M. Chiba, K. Uosaki, Optical recognition of surface chirality at Au(hkl) single crystalline surfaces by second harmonic generation rotational anisotropy [J], J. Am. Chem. Soc. 127 (2005) 12743–12746.
[5] G. Gubitz, M.G. Schmid, Biopharm. Chiral separation by chromatographic and electromigration techniques. A review [J], Drug Dispos. 22 (2001) 291–336.
[6] Y. Matsuoka, N. Kanda, Y.M. Lee, A. Higuchi, Chiral separation of phenylalanine in ultrafiltration through DNA-immobilized chitosan membranes [J], J. Membr. Sci. 280 (2006) 116–123.
[7] P. Jenner, B. Testa, The influence of stereochemical factors on drug disposition [J], Drug Metab. Rev. 2 (1974) 117–184.
[8] H.Y. Aboul-Enein, I.W. Wainer, The Impact of Stereochemistry on Drug Development and Use, Wiley, New York, 1997.
[9] H. Wan, L.G. Blomberg, Chiral separation of amino acids and peptides by capillary electrophoresis [J], J. Chromatogr. A 875 (2000) 43–88.
[10] Y. Kamatani, H. Minakata, P.T.M. Kenny, T. Iwashita, K. Watanabe, K. Funase, X.P. Sun, A. Yongsiri, K.H. Kim, P. Novalesli, E.T. Novales, G.G. Kanapi, H. Takeuchi, K. Nomoto, Achatin-I, an endogenous neuroexcitatory tetrapeptide from achatina fulica férussac containing A d-amino acid residue [J], Biochem. Biophys. Res. Commun. 160 (1989) 1015–1020.
[11] H. Bruckner, T. Westhauser, Chromatographic determination of D-amino acids as native constituents of vegetables and fruits [J], Chromatographia 39 (1994) 419–426.
[12] J.W. Daly, J. Caceres, R.W. Moni, F. Gusovsky, M. Moos, K.B. Seamon, K. Milton, C.W. Myers, Frog secretions and hunting magic in the upper Amazon: identification of a peptide that interacts with an adenosine receptor [J], Proc. Natl. Acad. Sci. U. S. A. 89 (1992) 10960–10963.
[13] M. Wcisłoa, D. Compagnoneb, M. Trojanowicz, Enantioselective screen-printed amperometric biosensor for the determination of D-amino acids [J], Bioelectrochemistry 71 (2007) 91–98.
[14] Y. Kong, J.H. Ni, W.C. Wang, Z.D. Chen, Enantioselective recognition of amino acids based on molecularly imprinted polyaniline electrode column [J], Electrochim. Acta 56 (2011) 4070–4074.
[15] X.L. Yin, J.J. Ding, S. Zhang, J.L. Kong, Enantioselective sensing of chiral amino acids by potentiometric sensors based on optical active polyaniline films, Biosens. Bioelectron. 21 (2006) 2184–2187.
[16] M. Chen, Y.Z. Fu, X. Cui, L.L. Wang, Comparative analysis of proline enantiomer in chiral recognition of biological macromolecule in immunoassay [J], Electroanalytical 21 (2009) 2339–2344.
[17] A. Leitner, W. Lindner, Functional probing of arginine residues in proteins using mass spectrometry and an arginine-specific covalent tagging concept [J], Anal. Chem. 77 (2005) 4481–4488.
[18] H. Nakamura, T. Saheki, S. Nakagawa, Differential cellular localization of enzymes of L-arginine metabolism in the rat brain [J], Brain Res. 530 (1990) 108–112.
[19] G. Li, S. Regunathan, C.J. Barrow, J. Eshraghi, R. Cooper, D.J. Reis, Agmatine: an endogenous clonidine-displacing substance in the brain [J], Science 263 (1994) 966–969.
[20] A. Calver, J. Collier, P. Vallance, Dilator actions of arginine in human peripheral vasculature [J], Clin. Sci. 81 (1991) 695–700.

[21] R. Haggenmueller, H.H. Gommans, A.G. Rinzler, J.E. Fischer, K.I. Winey, Aligned single-wall carbon nanotubes in composites by melt processing methods [J], Chem. Phys. Lett. 330 (2000) 219–225.
[22] M.D. Frogley, D. Ravich, H.D. Wagner, Mechanical properties of carbon nanoparticle-reinforced elastomers [J], Compos. Sci. Technol. 63 (2003) 1647–1654.
[23] Y.L. Cao, R. Yuan, Y.Q. Chai, L. Mao, H. Niu, H.J. Liu, Y. Zhuo, Ultrasensitive luminol electrochemiluminescence for protein detection based on in situ generated hydrogen peroxide as coreactant with glucose oxidase anchored AuNPs@MWCNTs labeling, Biosens. Bioelectron. 31 (2012) 305–309.
[24] R. Andrews, M.C. Weisenberger, C. Opin, Carbon nanotube polymer composites [J], Solid State Mater. Sci. 8 (2004) 31–37.
[25] B.G. Demczyk, Y.M. Wang, J. Cumings, M. Hetman, W. Han, A. Zettl, R.O. Ritchie, Direct mechanical measurement of the tensile strength and elastic modulus of multiwalled carbon nanotubes Mater[J], Sci. Eng. A 334 (2002) 173–178.
[26] J.M. Nugent, K.S.V. Santhanam, A. Rubio, P.M. Ajayan, Fast electron transfer kinetics on multiwalled carbon nanotube microbundle electrodes [J], Nano Lett. 1 (2001) 87–91.
[27] S. Ravindran, S. Chaudhary, B. Colburn, M. Ozkan, C.S. Ozkan, Covalent coupling of quantum dots to multiwalled carbon nanotubes for electronic device applications [J], Nano Lett. 3 (2003) 447–453.
[28] C. Richard, F. Balavoine, P. Schultz, T.W. Ebbesen, C. Mioskowski, Supramolecular self-assembly of lipid derivatives on carbon nanotubes [J], Science 300 (2003) 775–778.
[29] A. Salimi, R. Hallaj, Catalytic oxidation of thiols at preheated glassy carbon electrode modified with abrasive immobilization of multiwall carbon nanotubes: applications to amperometric detection of thiocytosine, L-cysteine and glutathione [J], Talanta 66 (2005) 967–975.
[30] Y.Z. Fu, M. Chen, X. Cui, L.L. Wang, Q. Chen, J. Zhou, Recognition behavior of chiral nanocomposites toward biomolecules and its application in electrochemical immunoassay [J], Sci. Chin. Chem. 53 (2010) 1453–1458.
[31] M.O. Finot, G.D. Braybrook, M.T. Mcdermott, Characterization of electrochemically deposited gold nanocrystals on glassy carbon electrodes [J], J. Electroanal. Chem. 466 (1999) 234–241.
[32] Y. Zhuo, P.X. Yuan, R. Yuan, Y.Q. Chai, C.L. Hong, Nanostructured conductive material containing ferrocenyl for reagentless amperometric immunosensors [J], Biomaterials 29 (2008) 1501–1508.

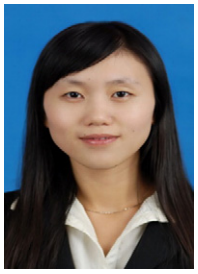

Qiao Chen is a MS candidate in the College of Chemistry and Chemical Engineering of Southwest University, China, is interested in the development of electrochemical devices for chiral biosensors.

Min Chen is a MS candidate in the College of Chemistry and Chemical Engineering of Southwest University, China, is interested in the development of electrochemical devices for chiral biosensors.

Juan Zhou is a MS candidate in the College of Chemistry and Chemical Engineering of Southwest University, China, is interested in the development of electrochemical devices for chiral catalysis and analysis.

Qian Han is a MS candidate in the College of Chemistry and Chemical Engineering of Southwest University, China, is interested in the development of electrochemical devices for biosensors and chiral analysis.

Yonghua Wang is a MS candidate in the College of Chemistry and Chemical Engineering of Southwest University, China. Her major interests are the development of electrochemical chiral sensor.

Yingzi Fu is a professor of chemistry in Southwest University, China, received PhD degree in analytical chemistry from this University in 2006. The main research interests are nanomaterials, biosensors and electrochemical chiral recognition.